

IXO X-Ray mirrors based on slumped glass segments with reinforcing ribs: optical and mechanical design, image error budget and optics unit integration process

M. Civitani^{a1}, S. Basso^a, M. Bavdaz^b, O. Citterio^a, P. Conconi^a, D. Gallieni^c, M. Ghigo^a, B. Guldemann^b, F. Martelli^d, G. Pagano^a, G. Pareschi^a, G. Parodi^d, L. Proserpio^a, B. Salmaso^a, D. Spiga^a, G. Tagliaferri^a, M. Tintori^c, E. Wille^b, A. Zambra^a

^aINAF-OAB Astronomical Observatory of Brera, Via E. Bianchi 46, I-23807 Merate (LC), Italy

^bEuropean Space Agency, ESTEC, Keplerlaan 1 - P.O.Box 299, NL -2200AG Noordwijk, The Netherlands

^cA.D.S. International, Via Roma, 87 – I-23868 Valmadrera (LC), Italy

^dBCV-Progetti, Via S. Orsola 1, I-20123 Milano, Italy

ABSTRACT

The International X-ray Observatory (IXO) is being studied as a joint mission by the NASA, ESA and JAXA space agencies. The main goals of the mission are large effective area ($>3\text{m}^2$ at 1 keV) and a good angular resolution (<5 arcsec HEW at 1 keV). This paper reports on an activity ongoing in Europe, supported by ESA and led by the Brera Astronomical Observatory (Italy), aiming at providing an alternative method for the realization of the mirror unit assembly. This is based on the use of thin glass segments and an innovative assembly concept making use of glass reinforcing ribs that connect the facets to each-other. A fundamental challenge is the achievement with a hot slumping technique of the required surface accuracy on the glass segments. A key point of the approach is represented by the alignment of the mirror segments and co-alignment of the mirror pairs assembled together. In this paper we present the mirror assembly conceptual design, starting from the design of the optical unit, the error budgets contributing to the image degradation and the performance analysis to assess error sensitivities. Furthermore the related integration concept and the preliminary results obtained are presented.

Keywords: IXO telescope, X-ray segmented optics, integration and assembly of glass foils for X-ray telescopes

1. INTRODUCTION

IXO is a joint X-ray observatory, with participation from ESA, NASA and JAXA, dedicated to deep imaging and high resolution X-ray spectroscopy, with 100 times the throughput of previous X-ray observatories (i.e. XMM Newton and Chandra). This mission supersedes the XEUS and Constellation-X mission concepts previously studied by ESA and NASA respectively. The current baseline for IXO features a single large X-ray mirror module and an extensible optical bench with a 20-25m focal length, with an interchangeable focal plane. Differently from XMM and Chandra, for such a big optics size it is impossible to rely on monolithic pseudo-cylindrical mirror shells, losing in that way the intrinsic stiffness coming from mechanical structures with cylindrical symmetry. Moreover, due to the mass limit imposed by the capabilities of launchers, IXO relies on a much more challenging ($\sim 17\text{ cm}^2/\text{kg}$) area-to-mass ratio. Finally, taking into account the huge reflecting surface of the optics, the mirror manufacturing process should be scalable to a high volume production industrial level with an affordable financial cost. For these reasons, since several years, ESA is pursuing the development of silicon pore optics as a candidate technology for the focusing optics of next generation X-ray space observatories [RD1]. In the mean time, the fabrication of large segmented optics based on thin shaped glass plates, obtained by hot slumping, was explored by US teams in the context of the development study of the Constellation-X mission and it is now also proposed for IXO [RD2]. While so far the two options were separately explored in parallel in Europe and US, recently a back-up study based on the thermally slumped glass technique is explored also in Europe, as a

¹ marta.civitani@brera.inaf.it; phone +39-039-5971089; fax +39-039-5971000; www.brera.inaf.it

risk mitigation measure. The present work is performed in the framework of a development study aiming at the production of a XOUI based on glass plates, to be integrated together using an innovative method [RD3]. In this paper we present part of the work that has been performed in the context of the ESA contract “Back-up IXO optics Technology” (started on September 2009) and, in particular, the mirror assembly conceptual design based on thin glass foils, starting from the design of the optical unit and from the error budgets contributing to the image degradation and the performance analysis to assess error sensitivities. Furthermore the related integration concept and the preliminary results obtained on samples developed in the first part of the program are presented. An overall overview of the on-going development program is described in another paper of this volume [RD4].

2. MECHANICAL VS OPTICAL DESIGN

The manufacture of the IXO mirror assembly based on glass slumping process relies on the principle of hierarchical integration. We start from a number of pre-shaped foils with parabolic (or hyperbolic) shape that are stacked and connected together through glued ribs, whose aim is to maintain the mirror foils in their mutual correct position. The proposed “X-ray Optic Unit” (hereafter XOUI) integration procedure requires parallel integration of both parabolic and hyperbolic stacks onto a common monolithic supporting structure, which will become part of the XOUI structure. The integration of the plate pairs is performed with high precision alignment in order to get the desired HEW performances. The XOUI, once qualified and calibrated, are integrated on ground onto petals that, on turn, will be assembled together to form the entire optics system of IXO.

In line with this integration process, the terminology hereafter reported has been defined:

- **Mirror Plate (MP):** Glass foil forming an azimuthal fraction of the parabolic or hyperbolic surface for a given shell with Wolter I configuration.
- **Plate Pair (PP):** Pair of Mirror Plates, one parabolic and one hyperbolic.
- **X-Ray Optical Unit (XOUI):** Elementary optical unit composed of stack of glass Plate Pairs connected each other by glued ribs. An outer structure allows the handling, calibration and connection to the Mirror Petal Structure.
- **Mirror Petal Structure (PS):** Intermediate Level Structure containing a number of XOUIs. Several PSs are needed to azimuthally cover the entire aperture of the IXO Telescope.
- **IXO Mirror Assembly (FMA):** The whole optics assembly of the satellite, comprising optical and structural parts i.e. Mirror Optical Bench (MOB) equipped with PSs (if any) populated with the XOUIs made by stacks of MPs.

The top level parameters considered for the optical and mechanical design of the IXO optics based on glass facets are reported in the following table.

Table 1. IXO Main requirements summary. (*At the moment of the preparation of the present paper ESA and NASA decided to modify the effective area requirement at 1.25keV which is now 2.5m²)

<i>Geometry</i>	<i>Wolter I</i>
<i>Focal length</i>	20 m
<i>Field of view</i>	18 Arcmin diameter
<i>Coating</i>	Iridium or Pt + C overcoating
<i>Radius of clear aperture</i>	0.25 – 1.90 m
<i>Total Mirror assembly mass</i>	2000 kg
<i>Effective area requirements*</i>	3.00 m ² @ 1.25 keV
	0.65 m ² @ 6.50 keV
	0.15 m ² @ 30.0 keV
<i>HEW (1keV) in FOV</i>	5 Arcsec

2.1 Mechanical design

In the present design it has been assumed that the shell radius should be between 250mm and 1900mm. As all the assumptions concerning mechanical and thermal loads are based on the silicon pore optics needs, the mechanical design with mass budget will be assessed in the next phase of the project. Indeed it has been verified that a reliable design of the XOUs may be for the glass solution characterized by the following features:

- 40 MS pairs 200 mm x 200 mm (Parabola + Hyperbola separated by a central gap of 20 mm) with a separation angle of 0 arcmin between a shell and the next one.
- MS glass foils 0.4 mm thick coated with Ir or Pt plus a C overcoating
- Five glass ribs (with variable thickness and width) equally distributed (every 40 mm) connecting each foil to the next one. (Average values are about 200mm x 2mm x 3mm)
- Machined ribbed glass back-planes
- External titanium frame with system of flexures decoupling module deformation from FMA primary structure (or petal) deformation.
- Bonded connections ribs-MS foils
- Bonded connections backplate-I/F frames

In the next figures it is reported a scheme of the IXO hierarchical concept. An XOUs is clearly shown: the machined ribbed glass backplanes are placed on the front and on the rear sides of the stacks closing the stack on both sides. In order to form the XOUs, the stacks of foils are connected to each other by glued ribs. These ribs will connect separately the plates in the parabola stack and in the hyperbola stack. Bonded connections allow the integration in the petal structure.

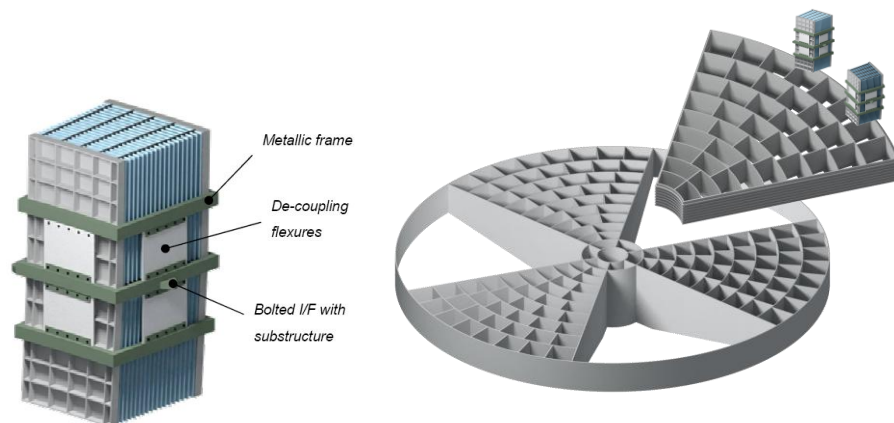


Figure 1. IXO Hierarchical concept

The lay-out of the optical units has been optimized by decreasing the unused area and keeping the proper azimuthally and radial spacing required for the arrangement of interfaces to substructure and substructure walls themselves. XOUs have been placed at radii down to ~0.25 m, while the maximum radius of the outermost MS at the interface approaches ~1.86m. The layout of the modules has been assessed considering a radial spacing between the optical units of about 40 mm and an azimuthal spacing of about 35 mm. These values (to be intended at hyperbola-parabola interface plane) represent the minimum spacing considered allowable for I/F accommodation; in addition they are assumed granting the adequate accessibility for regulations during integration phases. The adopted layout seems not to pose particular problems or challenges concerning petal walls and structures accommodation. Some preliminary analyses carried out for this purpose seem to confirm the assumption. For the present configuration the Mirror Assembly consists of 246 XOUs (41 XOUs for each petal) arranged in 9 nested rings. A list of materials envisaged for the design and adopted in the FEM are summarized in the following table.

Table 2: List of materials adopted in the analysis

<i>Component</i>	<i>Foreseen material</i>
XOU Mirror shells	Structural Glass: Schott D263T (or D263 ECO, TBD) Optical Coating: Iridium or Platinum
XOU Ribs	Structural glass: Schott D263T* (or D263 ECO, or BK7, TBD since at the moment D263 T and ECO is not produced with the required thickness).
XOU Backplate	Structural glass: see XOU ribs Depending on the specification on average operative temperature others materials could be envisaged.
Adhesive for XOU integration	Master Bond Polymer System EP30-2
XOU Case and I/F	Titanium Alloy Ti-15Mo-3Nb-3Al-0.2Si

**D263T has been adopted in the structural model even if not actually produced with required thickness; differences with BK7 mechanical properties seem negligible.*

2.2 Expected Effective Area

The optical design of the module is based on a Wolter I configuration and is actually determined by the dimensions of the segmented glass plate slumped (200 mm x 200 mm), their thickness (0.4mm), the gap length to be left at the intersection between the parabola and the hyperbola (20mm) and the acceptance angle between two adjacent shells (0 arcmin). Since for the innermost mirror shells the distance between two consecutive glass plates become small, it has been decided to set 1mm as the minimum thickness of the ribs. This choice should prevent from integration difficulties. The impact of the structure obscuration area has been analyzed with detailed ray-tracing simulations, in order to choose a design for the structure configuration compatible with the requirements for the Effective Area at different energies. The estimation of the effective area has been performed at @1keV, @4keV and @6keV. In the following pictures the cumulative effective area levels as a function of the shell indexes are reported, starting from the innermost shell. The different colors are related to the different rings of XOU used for the mechanical design. It should be noted that the vignetting due to the structure has been taken into account in the calculation. The requirements in terms of effective area are completely fulfilled considering a Pt coating with C over-coating.

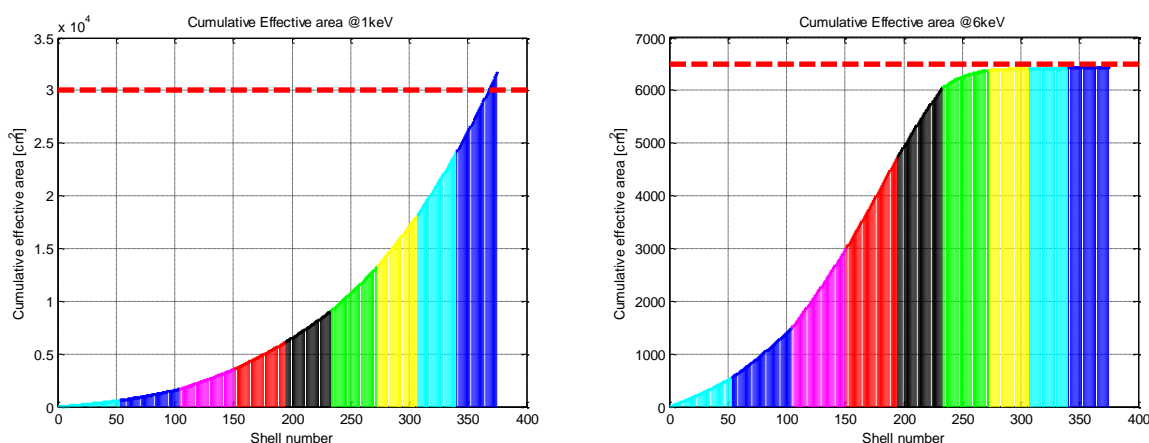


Figure 2. On the left, cumulative effective area @1keV. On the right, cumulative effective area @6keV [in red the requirement]

3. INTEGRATION CONCEPT AND RELATED ERROR BUDGET

The integration concept is based on the fundamental assumption that under a vacuum suction the plate can assume the shape of the forming mould. If the mould profile was previously precisely figured to the negative shape of the reflecting surface to be achieved, the glass plate fixed in this configuration has the ideal shape and, gluing the ribs as spacers between consecutive glass plates, can be integrated in the stack. These ribs will guarantee the strength of the XOUs and keep the plates in the right position and shape. As we said the glass plates have previously been shaped with hot slumping. This in principle can be done on the same mould that will be used for integration. Residual differences between the shape of the slumped glass plate and forming mould, for example due to non optimal slumping process, may introduce deformations in the glass plate as spring back effect after the glass plate release.

In this paragraph we will present the mould integration concept and the measurement configuration that allow the determination of the position and attitude of mould optical surfaces in space.

3.1 The mould integration

In order to position the glass segments in the stack without introducing deformations, it is necessary to provide a suitable integration tool, specifically developed for the use with very thin glass foils. A trick to avoid the problem of deformations of the plate introduced during the integration is to fix the glass onto the precisely machined mould (it could be the same used for the hot slumping process) by vacuum suction. A general scheme of the process is reported on the left in the next figure. On the right it is shown an example of the realized vacuum suction configuration with the ribs aligned on top. In order to avoid deformations in the glass, particular care has to be taken in the cleaning in order not to entrap dust grain between the mould and the glass. As the dust presence is evidenced by the visible fringes on the glass, the glass configuration can be easily evaluated before the integration.

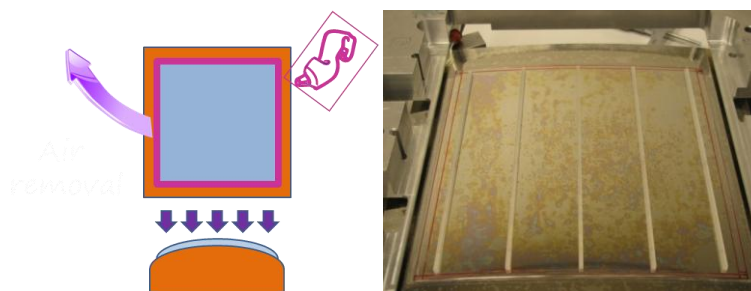


Figure 3. The glass plate under the effect of the vacuum suction assumes the shape of the mould. On the right an example of the development phase.

In this configuration the optical surface of the glass is kept in contact with the mould and the mould itself may be taken as a reference during the alignment of the plates in the stack. For this reason this integration scheme is called “mould integration”. Using the mould measurement, each plate pairs will be firstly aligned and then integrated into the stack by gluing it to the previous plate pair. In the next figures are reported the integration scheme of the plates in the stack and the mould measurement configuration selected.

It is important to point out that the adopted concept for the integration design does not need the machining of the ribs to precisely follow the curved rear of the figured glass plate surface. On the contrary the ribs will be just tapered to a coarse conical profile with differences $> 1 \mu\text{m}$ with respect to the curved surface; all the differences between ribs and glass profiles at macro and microscopic level will be compensated by the glue filling the gap. The idea is to align all the glass plates in the same stack with respect to a common reference system for the integration mould and filling under the applied vacuum suction the remaining gaps between ribs and foils with the glue. The glue thickness layer is around 50micron, which is not only able to absorb the differences from the desired and real profiles of the ribs but that also corresponds to the optimal values for the toughness and adherence of the glues (this aspect has been proven after careful experimental tests).

In order to align the plates in the stack, the parabola and hyperbola moulds are assumed as reference for the front reflecting surface of each plate. The position and the orientation of the moulds will be carefully measured with a 3d machine: these data will be used to align together the two moulds for parabola-hyperbola plates. The 3d machine ($1\mu\text{m}$

accuracy rms needed) measures the frame of the mould that is not covered by the glass plate. The output are the radii of curvature at the top and at the bottom of the moulds and the longitudinal profiles sampled with 1 mm steps. These outputs are used to find the best locations for the plate positioning/tilting, evaluated after a ray-tracing simulation.

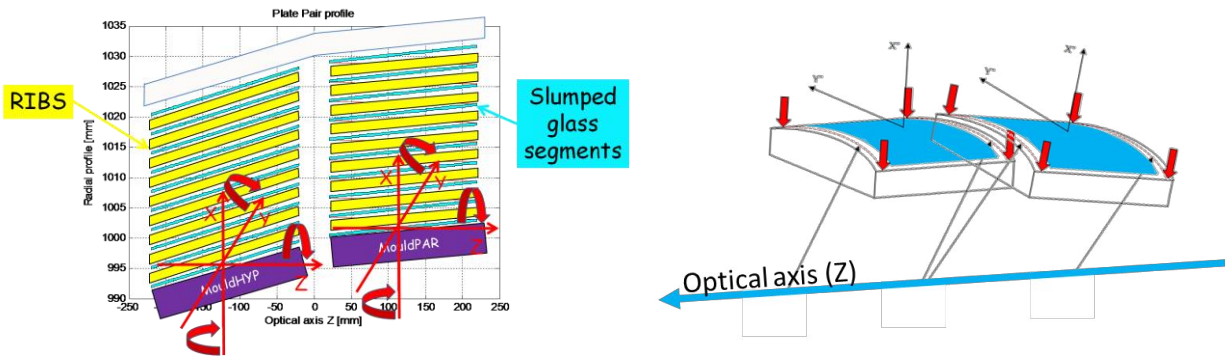


Figure 4. XOU mounting scheme and 3D measurement configuration.

It should be noted that this integration concept has the following advantages:

- The mould used for integration could be the same used for the slumping in the case of direct slumping process. In principle there is no need for additional integration tools and of markers for plate positioning, since it is already mounted on the mould. Nevertheless, the spring back effect due to a erroneous positioning is very small.
- The alignment of the optical surfaces of the two moulds during the integration could be also optimized to compensate possible mould errors manufacturing.
- The optical performances of the system during the Plate Pair (PP) integration can be evaluated (via ray-tracing) and kept under control during integration.

A simplification in the integration procedure could be the use of a monolithic mould of parabola and hyperbola. In this case the proposed integration scheme is still compatible, but with the difference that the relative orientation of the two plates will not be matter of integration but of mould realization. In fact, the tolerances on the position/attitude of the mould will be more relaxed but the mould requirement will be more tight. Instead in the baseline design, it will be the opposite as the integration may be used to correct mould realization errors.

3.2 XOU Error budget

In order to establish the feasibility of the XOU realization, an error budget has been built defining the tolerances of the various errors. These tolerances should include surface roughness, mirror plates figuring errors due to manufacturing errors, mechanical stresses at mirror module fixation point and mirror module thermal environment during operation. These requirements have also to cover the contribution of alignment errors between mirror plates in each mirror module and the contribution of alignment errors between mirror modules.



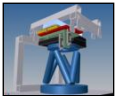
At the present stage of the project, we focused on the angular resolution performances @1keV: with an allocation of 2.8'' for the integration of the XOU in the bench structure of the FMA, the single XOU on-axis image quality need to be better than 4.3 arcsec. The single XOU error budget has been built considering the following categories of errors: i) mould realization errors, ii) errors induced by the replication process including errors due to the X-ray scattering (XRS) $HEW_{XRS}^2(\lambda)$ caused by surface roughness, iii) integration errors and iv) global errors effects on the FMA, v). With the contributions quadratically added, the requirements on the XOU can be written as:

$$HEW_{TOT}(\lambda) = \sqrt{HEW_{Mould}^2 + HEW_{RepProc}^2 + HEW_{Int}^2 + HEW_{GlobEff}^2}$$

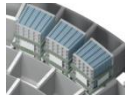
A first allocation budget for each term is given in next table. For each category the relevant contributors are highlighted. The XOU realization process has been divided into steps and for each kind of error an error allocation and the

corresponding tolerances are given. In the first column it is reported the total allocation for the category considering the double reflection. Clearly the partition is quite preliminary as some of the important contributes, e.g. slumping or gluing processes for example, need a careful experimental evaluation. The X-ray scattering term of the HEW at the photon energy of 1 keV for a double reflection and a XOu with ~1 m curvature radius and 20 m focal length can be directly computed from the power spectrum of the roughness of slumped mirrors [RD5]. Of course, other contributions could be considered. Nevertheless this preliminary partition is fundamental in order to finalize a reliable design of the Integration Machine to be used for the integration of the XOu.

Table 3. Preliminary Error budget table. All HEW errors in the first column should be added in quadrature.

HEW ERROR	ERROR DESCRIPTION	VALUE	TOLERANCES
	1,8'' MOULD FOR SLUMPING		
	Mould references (x2)	0.6	
	Average radius	0.1	0.2 mm
	Azimuth radius variation	0.1	0.5 mm
	Cone angle at Rmed	0.1	7"
	Cone angle variation with azimuth	0.1	0.5"
	Average Sag	0.4	30nm
	Sag variation with azimuth	0.4	30nm
	Profile errors (x2)	1.1	
	Tot Axial figure error (200-20mm)	0.7	0.06 µm
	Tot Axial figure error (20-2mm)	0.7	0.006 µm
	Tot Axial figure error (2mm-1micron)	0.5	5 Å
	3,5'' SLUMPING		
	Slumping accuracy(x2)	1.9	
	Dust		
	Glass thickness		
	Coating presences		
	Difference of temperature on the faces of the glass		
	Temperature uniformity on mould		
	Pressure uniformity		
	CTE influences		
	Differences between mould and glass CTE		
	Differences between coating and glass CTE		
	XRS AT 1 keV	2.3	
	1,5'' INTEGRATION		
	Mould Measurement (x2)	0.5	
	Glass positioning with respect the mould	0.1	0.5 mm
	Radius measurement	0.25	25 µm
	Optical axis rotation around Z	0.1	
	Optical axis rotation around Y	0.1	
	Optical axis rotation around X	0.1	0.5''
	Average slope measurement	0.4	0.2''
	Parabola Plate positioning	0.6	
	Par Displ along X	0.1	20 µm
	Par Displ along Y	0.1	20 µm
	Par Displ along Z	0.002	20 µm
	Par Rot. around X	0.16	1.00''
	Par Rot. around Y	0.5	0.25''
	Par Rot. around Z	0.125	10''
	Ribs gluing	0.5	
	Positioning of the ribs		
	Gluing ribs over mould		
	PP couple positioning	0.1	

HEW ERROR	ERROR DESCRIPTION	VALUE	TOLERANCES
	PP displ. Al. X	0.1	5 μm
	PP displ. Al. Y	0.1	5 μm
	PP displ. Al. Z	0.005	5 μm
	PP rot. Ar. X	0.0	20''
	PP rot. Ar. Y	0.0	20''
	PP rot. Ar. Z	0.0	20''
	Integration on Backplane	1.0	
	Gluing on backplane		
	Vacuum release		
2,8''	GLOBAL EFFECTS		
	Gravity effects	2.0	
	Gravity effects		
	Thermal gradient	2.0	
	Glue thermal effects		
	Axial temperature gradient		
	Transverse temperature gradient		
	Vertical temperature gradient		
5''	TOTAL: XOU INTEGRATED IN FMA		



In the following paragraph the various errors contribute are highlighted and criticality analyzed.

4. ERRORS SENSITIVITY ANALYSIS

In this paragraph the sensitive analysis on the possible errors that can occur in the process is reported. In the case of the integration with 3D metrology machine, the integration process errors considered will be: a) Slumping errors, b) Plates positioning on the moulds, c) Parabola and Hyperbola position/orientation, d) PP position/orientation, d) Measurement errors, e) Ribs Gluing errors, f) PP Gluing to backplane, g) Vacuum release. The sensitivity error analysis has been carried out when possible through ray tracing and FEA simulations. The knowledge about some other contributors is under experimental evaluation with dedicated test, as for example for the slumping process. Test dedicated to characterize the glue effects will be subject of a dedicated paper.

4.1 Mould Errors sensitivity analysis

The first term of the error budget concerns the error of the forming moulds, used to slump the plates. Assuming that the glass foil copies the shape of the mould, possible sources of errors are listed hereafter:

- Average radius. Assuming that the plate glass has the same average radius of curvature of the forming mould, if a plate glass with an error on the average radius is placed at the nominal value for the radius, some distortions of the optical figure are expected.
- Average cone angle. This contributor is equivalent to a focal change. It can be partially corrected, tilting the plate in the opposite direction. This correction introduces some distortions in the optical figure.
- Average Sag. The sensitivity to this kind of error is large. As for plate with a radius of curvature of 1m the sagitta is $\sim 0.78 \mu\text{m}$, an error of this order would be equivalent to consider a double cone configuration, with an $\text{HEW} = (R_{\text{max}} - R_{\text{med}})/2 = 12.5''$

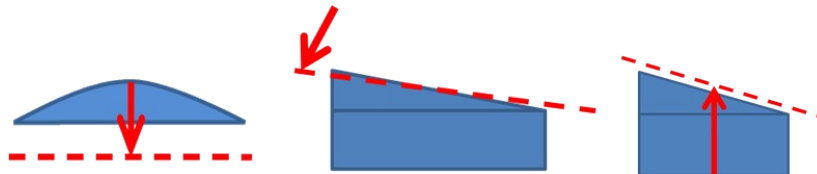


Figure 5. Mould errors schematics

In order to correct these average errors during integration, the as-manufactured radius and cone angle should be within tolerances and the accuracy of their measurement should be of the same order. For the remaining distortions of the resulting optical figure, an allocation in the error budget is foreseen.

In addition to these errors, the variation along the azimuth of the radius of curvature, cone angle and sag should be considered. Moreover, the main contributors remain the profile errors along the optical axis, assuming that the slumping process will copy these errors on the plate.

Average Radius

In order to define the tolerances on the average radius of curvature of the slumping mould, ray-tracing simulations are performed. For simplicity, the two plates are assumed to be in contact at intersection plane. Firstly, it is considered the case of an error on the parabola average radius. Assuming the parabola to be integrated in the nominal position, the HEW is calculated. For a radius of curvature with an error of +1mm, the HEW increases by $\sim 0,5''$. Then, it is considered the case in which the radius of the hyperbola is different from the theoretical value. If this mould is placed in the theoretical position it should have, a degradation of the focal spot HEW is observed. Also in this case the HEW increases by $\sim 0,5''$ for a radius of curvature with an error of +1mm. The tolerances imposed on the average radius of the mould are derived from the HEW degradation. The dependence is linear and can be described as:

$$HEW_{AveRadiusError} = k \Delta R,$$

with $k = 0.5''/\text{mm}$, assuming a contribution of $0.1''$ to the HEW, the requirement on the average radius is 0.2 mm.

Cone angle

The mould can have an error on the cone slope. This error has an impact in terms of both HEW and focal spot baricentre displacement. This effect may be corrected during integration phase along with a rotation of the plate.

The HEW contributors are reported hereafter:

$$HEW_{AveConeAngle} = Cost_{HEW} * SlopeError$$

$$BAR_{AveConeAngle} = Cost_{BAR_X} * SlopeError$$

with $Cost_{HEW} = 0.15$ and $Cost_{BAR_X} = 2$. When a cone angle error is measured, it is possible in principle to correct for it with a rotation of the plate. In the following figure is reported the case in which the correction of the parabola tilt is done assuming cone angle error of $10''$. As can be seen, with a correspondent tilt of the parabola it is possible to recover easily the HEW contributor. In contrast, bringing the image baricentre back to the nominal position is more difficult. In fact an error of $0.5''$ in the tilt prevents us to bring the baricentre to less than $1''$ from the nominal position.

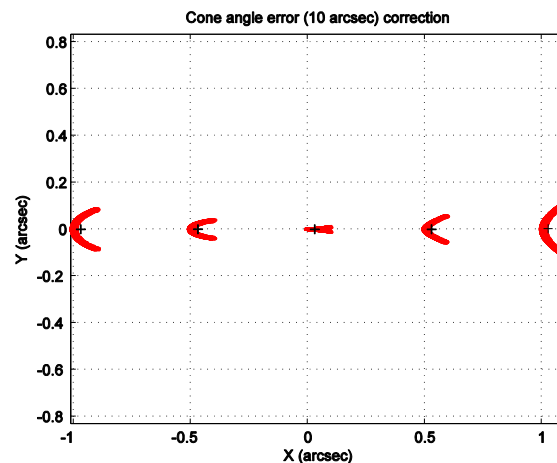


Figure 6. Parabola cone angle error compensation with parabola plate tilt around Y. The focal spot corresponding to $9.5''$, $9.75''$, $10''$, $10.25''$ and $10.5''$ is reported.

Average sag

When an error on the average sag is present on the mould, it contributes to change the shape of the focal spot and therefore its HEW. With a tolerance of 50nm on the parabola sag, the contribution to the HEW is around $0.4''$.

4.2 Plates alignment sensitivity analysis

In this analysis the parabola and hyperbola plates are assumed without figure errors. Only one of the two is rotated each time around the different axis with the centre of rotation correspondent to the centre of the plate as shown in the next figure for the parabola.

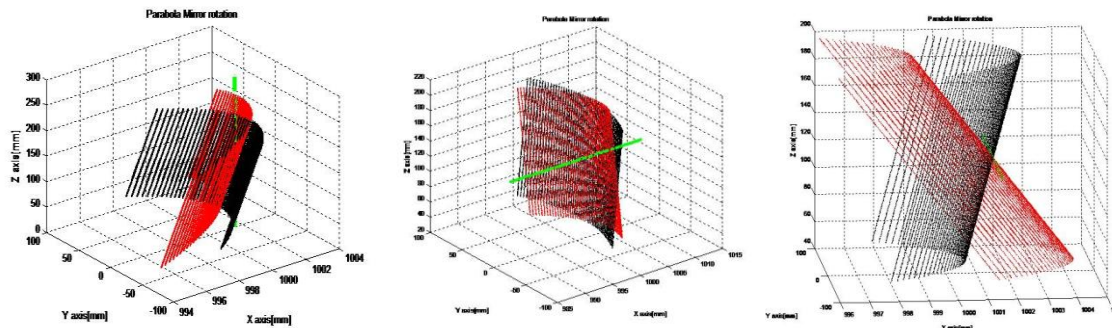


Figure 7. Rotation of the plates with respect to the axis

In correspondence to the displacements and rotations of the plates, the degradation on the focal spot can be either a simple focal spot degradation or a displacement of the focal spot baricentre. When this effect is observed, it is more important of the focal spot aberration and sensitivities are given in terms of this contribution.

In the following table are reported the sensitivities of the alignment errors: in the comments column is reported if there is a displacement of the focus and in which direction.

Table 4. Integration of a glass plate

<i>CONTRIBUTORS</i>	<i>HPD SENSITIVITY</i>	<i>COMMENTS</i>
PAR alignment		
Par. Displ al. X	$0.5''/0.1\text{mm}$	Focal spot baricenter displacement along X direction
Par. Displ al. Y	$0.5''/0.1\text{mm}$	Focal spot baricenter displacement along Y direction
Par. Displ al. Z	$0.01''/0.1\text{mm}$	Focal spot baricenter displacement along X direction (F# depending) $0.1''/F\# \times 0.1\text{mm}$.
Par. Rot ar. X	$1.6''/10''$	Focal spot aberration
Par. Rot ar. Y	$20''/10''$	Focal spot baricenter displacement along X direction
Par. Rot ar. Z	$0.25''/10''$	Focal spot baricenter displacement along Y direction
HYP alignment		
Hyp. Displ al. X	$1.5''/0.1\text{mm}$	Focal spot baricenter displacement along X direction
Hyp. Displ al. Y	$0.5''/0.1\text{mm}$	Focal spot baricenter displacement along Y direction
Hyp. Displ al. Z	$0.05''/0.1\text{mm}$	Focal spot baricenter displacement along X direction (F# depending)
Hyp. Rot ar. X	$1.6''/10''$	Focal spot aberration
Hyp. Rot ar. Y	$20''/10''$	Focal spot baricenter displacement along X direction
HYp. Rot ar. Z	$0.25''/10''$	Focal spot baricenter displacement along Y direction

As can be seen, severe contributors are the alignment of the plate around axis Y, that contributes with a focal spot displacement of $2''/1''$ rotation and around X that contributes with a focal spot aberration of $1.6''/10''$ rotation.

On the contrary, in the case of plate pairs couple rotation, the sensitivity analysis results are more relaxed. In the next figure is reported for example the rotation of a couple of plate pairs around the different axis.

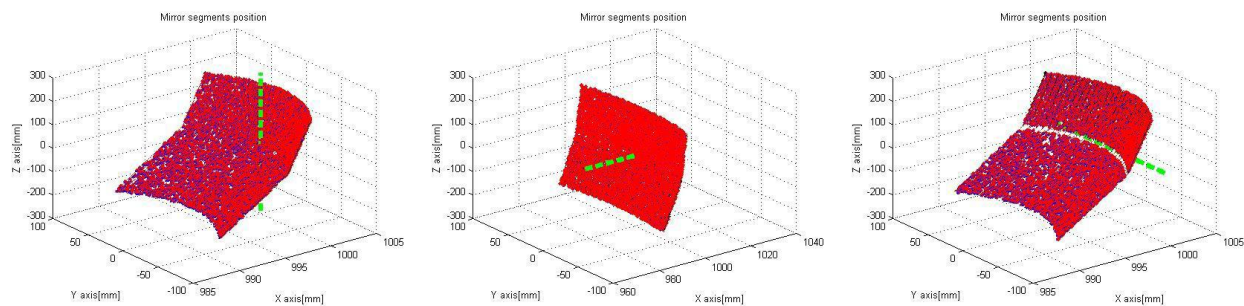


Figure 8. Axis used for PP rotations

Results of this sensitivity analysis are reported in the next table.

Table 5. Integration of the plate pair couple

<i>CONTRIBUTORS</i>	<i>HPD SENSITIVITY</i>	<i>COMMENTS</i>
PP displ. Al. X	1''/50 μ m	Baricentre displacement
PP displ. Al. Y	1''/50 μ m	Baricentre displacement
PP displ. Al. Z	1''/1 mm	Baricentre displacement, shell dependent
PP rot. Ar. X	0.013''/10''	Baricentre displacement along X
PP rot. Ar. Y	0.002''/100''	Focal spot Aberration
PP rot. Ar. Z	0.1''/10''	Focal spot aberration, radius dependent

4.3 Mould Measurement with 3D machine

Assuming the moulds have been already measured, basic information (average cone angle, average radius, average sag) of the mould geometry useful for the integration are already known. As we said, during integration, with the plate glass fixed on the mould under vacuum pressure, the two moulds are measured with a 3D machine. Due to space limitations, the accessible faces of the mould are on the top, at the bottom and on the sides of the glass plate.

- For each plate a scan is performed on the top and on the bottom of the mould accessible surface. The expected measurement duration is estimated in 10 min for each scan, assuming a sampling of 1 mm.
- The measurement scan data should be analyzed in order to determine the optical axis of each mould/plate.
- Each scan can be repeated to decrease the measurement errors.

From these measurements the expected information on the moulds position and orientation are:

- Radius of curvature.
- Position of the moulds along Z.
- Position of the moulds along X and Y.
- Optical axis rotation around X and Z.
- Plate orientation around Y.

Obviously the performances of this measure are increased if the mould geometry has already been measured, and therefore it can be used as a reference. Instead, if we assume that we do not know the intrinsic geometry of the mould, the search for these parameters will be a blind search. Hereafter are reported the calculation relevant to this second case. The radius of curvature determination is quite accurate using the data from the scan: in particular it depends strongly on the width of the arc of circumference. For example, the results obtained from a measurement on an angular width of 8.5°

are reported in the next figure. In this case, the measurement accuracy can be upgraded only repeating the measure. In order to reach the tolerances of 25 μm , the measure should be repeated about 10 times.

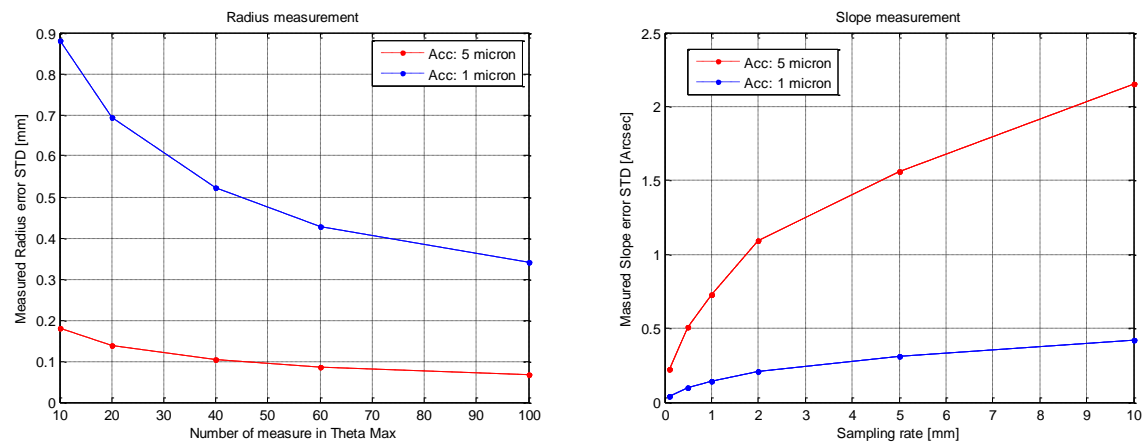


Figure 9. On the left STD for the measured radius of curvature from the data of one scan. On the right Standard deviation of the average slope as measured from a profile on the side of the plate for different 3D machine accuracy.

From the measurement of the top and bottom parts of each mould, once the centre of curvature is determined it is possible to establish if the optical axis is misaligned with respect to the 3D machine reference system. From the data along the side of the plate glass, it is possible to calculate the average slope of the segment. In the above figure is reported the standard deviation for a 3D machine with an accuracy of 1 μm or 5 μm . With a sampling rate below 1mm and an accuracy of 1 μm , the standard deviation of the measured slope is around 0.1''.

Table 6. The STD of the measured radius and rotation angles around X and Y.

<i>NUM. OF MEASURE</i>	<i>SAMPLING STEP</i>	<i>RADIUS STD</i>	<i>ROT. AROUND X</i>	<i>ROT. AROUND Y</i>
200	1 mm	17 μm	0.8''	26''
400	0.5 mm	12 μm	0.6''	18''

As previously anticipated, the complexity of the two moulds alignment can be reduced using a monolithic mould, instead of separate parabola and hyperbola moulds: in this case the two plates will be fixed in the desired position on the monolithic mould and integrated as in normal case. In this configuration, the integration is really simplified as the alignment as well its stability during glue curing is not necessary. On the other hand, the tolerances on the mould realization are tighter as the relative angles between the two cone angles have a non-negligible impact on the optical performances. In the next pictures are reported the effects at the focal plane of an error of 1mm radius of curvature on the parabola + hyperbole mould. This error is the linear sum of what one found for the case of parabola and hyperbole mould. Moreover, an error on the relative angle between the two cones will result in a change of focal length with a displacement of the focal spot. While this kind of error can be recovered in the case of separate moulds for a monolithic mould this is not possible. In the figure is reported in blue a tentative compensation of the error with a tilt of the couple. Although exaggerated, it is still not sufficient.

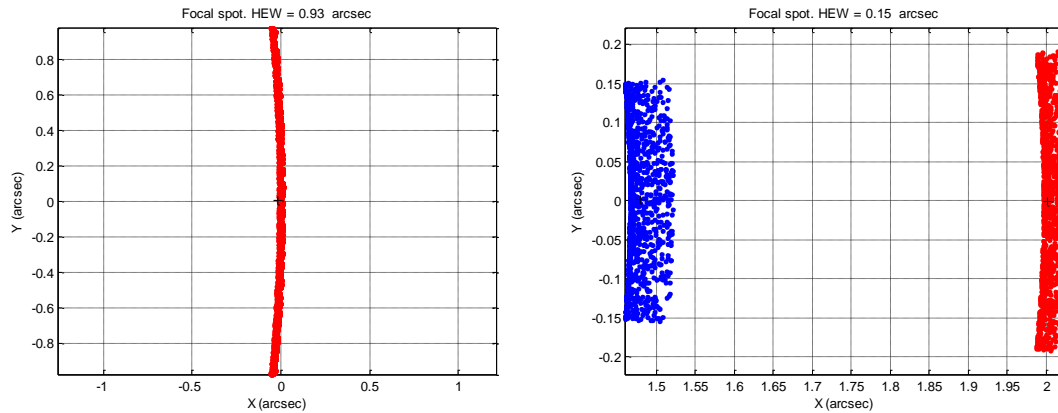


Figure 10. On the left the error of 1mm in the radius of curvature on the parabola + hyperbola mould. On the right the effect of an error of 1'' on the slope of parabola cone with respect to the cone (in blue the failed correction with 100'' tilt)

4.4 Glass plates alignment on the mould

If there is an error on the plate positioning with respect to the mould, the situation will be the following:

- mould are aligned
- plates are forced into the mould shape with vacuum

These conditions mean that the glass plate will have the correct shape for a Wolter-I, at least until the vacuum release, but due to the misalignment, probably there will be a reduction in the effective area. As this error will be less than 1mm, the effective area reduction is in any case less than 1%. At the release of the vacuum, spring-back effects are possible and would affect the shape of the plate.

As the differences in shape between a misaligned plate and a well-aligned plate on the mould are of the order of tens of nanometer, the effect is considered negligible. In summary if we had a successful 'Mould integration', the possible effects are:

- Effective area loss (\rightarrow tolerable less than 1%)
- Spring-back effect of the stressed glass plate forced in not proper position (\rightarrow tolerable less than 0.5'')

The tolerances on the plate positioning with respect to the mould are fixed to 0.5 mm.

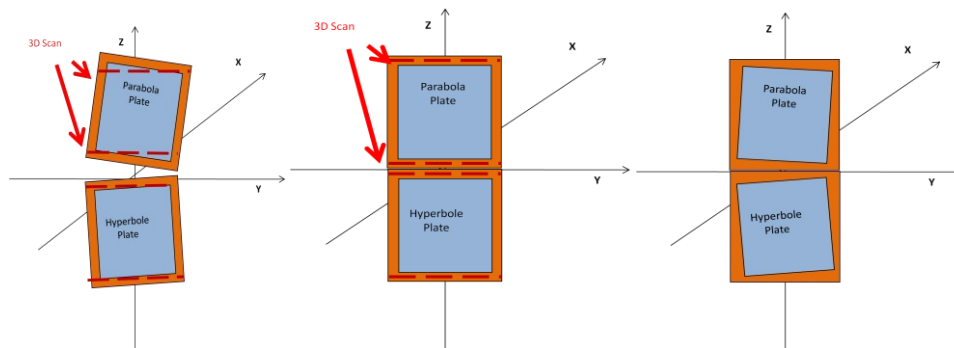


Figure 11. Incorrect alignment effects scheme

4.5 Gluing errors

Ribs are glued between two consecutive plates to maintain shape and mutual position of mirrors and to guarantee the stiffness of the system. For these reasons the selected material is the glass, in order to avoid problems with CTE mismatch. To be compatible with the optical design and to avoid the necessity of shaping the ribs, the main characteristics of the glass-glass bonding is that differences in glue thickness should not affect the shape of the glass

plates. As of today, the design of the ribs foresees thickness variations less than 10 μm . In order to fulfil this main requirement the glue should have very low shrinkage. The glue should respond to the following request to be compatible with the mechanical/optical design:

- Strength compatible with loads expected on the bonds
- CTE compatible as much as possible with glass (D263)
- Very low level of shrinkage
- Low outgassing

The selected glue for phase A is epoxy Masterbond EP30-02. The main characteristics given in the datasheet are reported in next table.

Table 7. Main glue characteristics (datasheet)

<i>Parameters</i>	<i>Value</i>	<i>Comments</i>
Tensile strength, ultimate 75°F	11,300 psi	
Compressive strength, ultimate,	>10,000 psi	
Thermal expansion coefficient 75°F	40-45 $\times 10^{-6}/^{\circ}\text{C}$	
Shrinkage upon cure	0.0003 inch/inch.	exceptionally low

Nevertheless, the datasheet values are promising for our needs but have to be confirmed by specific tests. Thermo-mechanical proprieties of the glue are under evaluation with specific tests. The glue shrinkage effects are under evaluation on flat samples and stack. Results on these topics will be presented in future papers.

4.6 Slumping errors and vacuum release

In the error budget it is foreseen a contribution from the slumping errors: thermal distortions due to temperature gradients or due to CTE mismatch of the different materials involved in the slumping process may cause errors in the shape of the glass plates.

The integration concept proposed allows for the partial correction of these errors. In fact, before the integration the MS is forced by vacuum against a mould having the correct shape and so eventual glass plate errors are corrected with elastic deformations. Then the MS is glued to the XOU ribs and the mould is released. The glued connections to the ribs partially freeze the plate shape but some spring back, due to stored elastic energy, is expected. Due to the rib presence the spring back now operates on a different constraint configuration, so the final plate error will have different shapes, with smaller spatial scale, related to the rib spacing. The phenomenon is governed by: the mechanical properties of plates material, their dimensions and thickness, the plate curvature radius, the shape and amplitude of the original plate shape error at the end of the slumping process and finally the rib number (and therefore the rib spacing). In the following three different plates shape errors are considered, corresponding to first order developed error terms: in the pictures the error is represented with magnified scale. The final residual MS shape errors at the integration end is also reported for the three cases. Red zones represent maximum positive errors (outwards) while blue zones represent maximum negative values (nearly zero error in case #2). Pictures are relevant to the nominal case having 5 ribs.

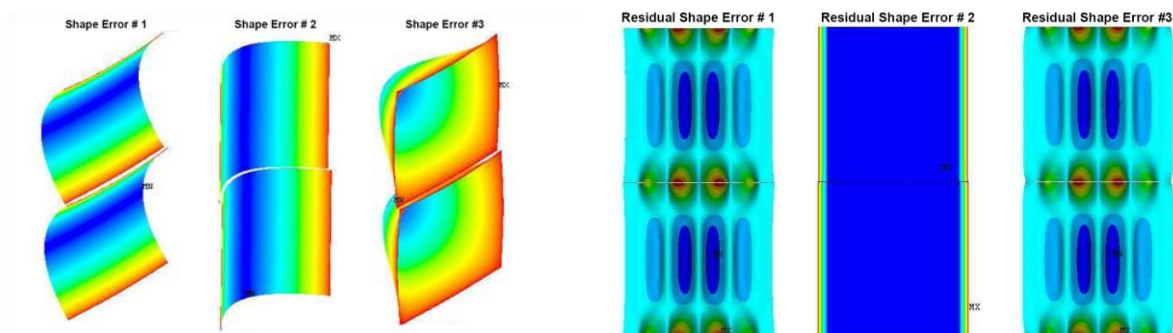


Figure 12. On the left the Errors considered while on the right the resulting shape of the glass after the integration. The error amplitude is equal to 10micron for shape errors #1 and #3, while for shape error #2, which has much lower effects, an initial amplitude equal to 100micron has been used.

In the table below the FEA results are summarized for plates having radius at the parabola-hyperbola interface respectively equal to 250, 1000 mm and 1900 mm considering the same longitudinal error amplitude of 10 micron.

Table 8. Integration Correction percentage for case #1

<i>RADIUS</i> [MM]	<i>HEW</i> <i>BEFORE</i> [ARCSEC]	<i>PV</i> <i>AFTER</i> [μM]	<i>HEW</i> <i>AFTER</i> [ARCSEC]	<i>CORR.%</i>
250	142.21	6.81	12.49	31.9%
1000	156.78	1.77	3.19	82.3%
1900	161.94	0.61	1.05	93.9%

For each case the glass plate errors are reported both in terms of peak to valley (PV) error and corresponding HEW. In the last column is given the error correction percentage (in terms of PV with respect to the initial error of 10μm). As the correction of error shapes #1 and #3 is carried out on a much more stiff structure, due to the plate curvatures in azimuthal plane, their shape errors are much more severe with respect to shape error #2. For the same reason plates having larger curvature in azimuthal plane (R=250mm) shows larger degradation under the same shape error amplitude. Even if the problem is not strictly linear, a first estimate of the HEW generated by spring back distortions can be carried out by assuming a linear trend of the HEW vs. the initial error amplitude. Assuming the same initial amplitude of the plate shape errors, the correction factor may be enhanced with an increase of the glass thickness or of the rib number, but at the present stage of the project they will not be considered as they involve a mass increase.

The experimental evidence of the correction capability of the proposed integration scheme is given in the following example. A slumped glass with quite an important sag error (~80 μm), measured at 45 mm from its longitudinal axis has been integrated on a rigid glass backplane with 5 ribs and ~50 μm of glue. The adopted integration procedure, followed in this first part of the project, is reported in the next figure and is based on the use of an integration jig. This jig allows maintaining the distance between the backplane and the ribs or between the ribs and the glass. Once fixed this distance, the gap in between is filled with the glue. The amount of glue distributed is calibrated to get the desired volume over the ribs and not to exceed the rib surface.

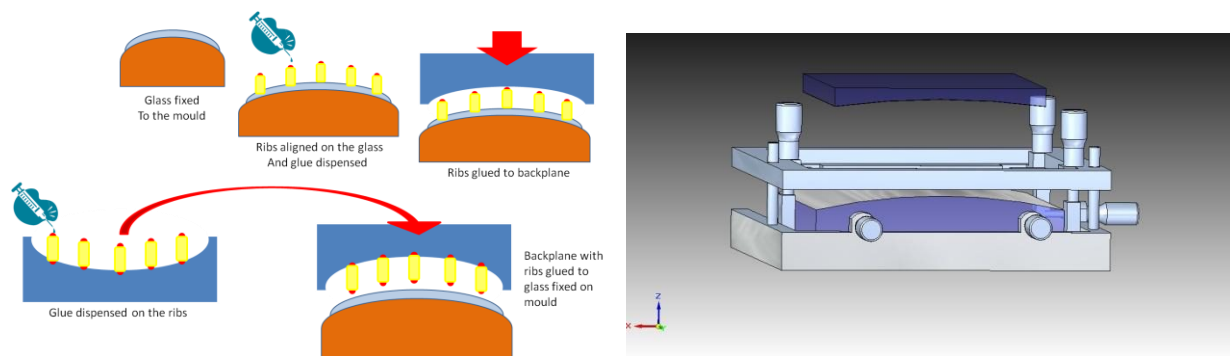


Figure 13. On the left the adopted integration procedure for the integration of single slumped glasses. On the right a scheme of the integration jig.

The resulting measure of the integrated glass is reported hereafter. In the figure is reported the 3D map [RD5] of the residual with respect to the best-fit cylinder. The ribs positions are clearly visible on the surface and in between them the glass deformation due to the spring back effect. Comparing the glass sag, roughly at the same axial distance, the profile error of the glass is reduced with a maximum sag of ~5 μm. This result is in line with the FEM simulations.

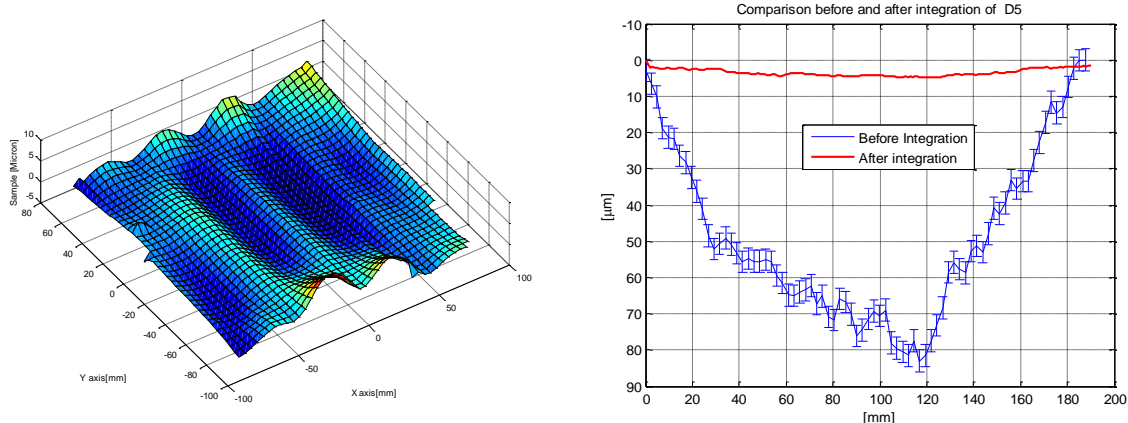


Figure 14. On the left the shape measurement of a slumped glass once Integrated on a rigid backplane. On the right the comparison of the sag error before and after integration at the same axial distance.

5. INTEGRATION MACHINE (IMA)

In order to carry out the integration of plates pair into the XOU a dedicated Integration Machine (hereafter IMA) has been designed, in accordance with the integration process and the corresponding error budget presented in the previous paragraphs. The IMA will align two separate moulds carrying each one its glass plate and then place at the same time the couple in position for their integration into the XOU. In the following is given an overview of the system.

5.1 IMA overview

The most demanding requirement that drives the design of the IMA is the relative attitude between the two moulds to be better than 0.25 arcsec around the around the Y axis. Such an angle must be kept constant across the overall curing time for gluing the ribs to the plates, which amounts to several hours. An attitude error of 0.2 μm on a 200 mm baseline corresponds to ~ 0.2 arcsec error: the two moulds have to be kept aligned better than this level. Even assuming a rigid temperature control of the integration environment, the differential thermal deformations of the mould and mirror module support structures could introduce attitude errors well above the allowed ones. For example, a Δ_{CTE} of 10 ppm on a 20 mm piece makes 0.2 μm for 1 C, which corresponds to 0.4 arcsec on a 100 mm baseline. In order to reach such a demanding specification, the active control of the relative attitude of the two moulds during the integration time has been considered the most appropriate approach. The problem is then moved to the implementation of actuators and feedback sensors with an adequate accuracy. Two more factors affect the active control system design. The overall stiffness (active and passive) of the mould mounts shall be consistent with the maximum loads introduced by the gluing process. On the other hand, the feedback sensors shall assure a long term stability consistent with the mould attitude prescription. As the idea of relying on the sensors stability does not work, this problem can be overcome by making differential measures of the moulds angles in a short time and to compare these data with a prescribed value. This is the design choice adopted and reported in the next section.

The Integration Machine has been designed to be as “flexible” as possible. The design of the IMA has to allow the use of separate PAR and HYP moulds to integrate the Plate Pair at the same time. This requirement led to a design with the following controls:

- Picomotors, used to reach the very fine alignment of the relative angles between the parabola and hyperbola moulds;
- Autocollimators, used to check the relative angle between the PAR and HYP moulds during the glue curing;
- Hexapod, used to perform the “macro” movements of the moulds pair. With respect to the common backplane.

For the mould integration monolithic case, the IMA could be modified and adapted just removing the picomotors and the autocollimators. In fact in this solution there is not the need to control such parameters because the relative alignment requirements are now on the mould manufacturing and not on the IMA. The position and attitude of the moulds are measured using a 3D measurement machine (UPMC) that has to be very precise (accuracy of 1 μm rms) in order to

properly align the moulds (and so the mirror glass). The first and third solution require better accuracy and resolution, while for the monolithic case the measures can have larger errors.

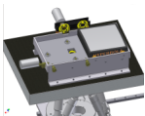
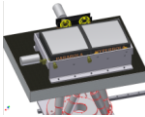
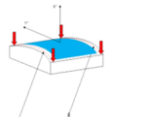
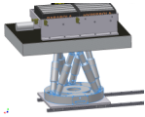
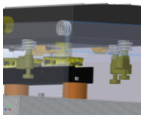
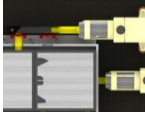
5.2 Design

The Integration Machine (IMA) is placed aboard a 3D measuring system (UPMC mod. 1200 CARAT by ZEISS) and organized in two stations. At the first place relative position and alignment of the two moulds is measured by the UPMC. The backplane for the plates pairs integration is placed at the second station: this is made by a “A” frame holding the backplane structure looking downward. A hexapod is mounted on a mobile frame that slides on linear ways switching among these two positions. The baseline choice for the hexapod is the model M-850 by Physik Instrumente (PI). The hexapod holds a rigid frame where the two moulds are mounted. The HYPerbola mould is fixed to the frame, while the attitude of the PARabola one is actively controlled through six actuators. Altogether the IMA has then 13 DoFs: the hexapod (6x), the moulds relative positions rotations (6x) and the station switcher (1x).

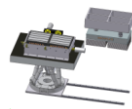
5.3 Integration steps

The description of the IMA functioning is given in the following section where the integration steps are reported.

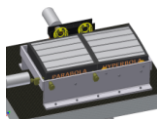
Table 9. Integration steps

IMAGE	STEP DESCRIPTION
	The HYP glass plate is mounted on its mould and held on it by vacuum suction; the alignment of the glass plate on its mould is done by markers with a typical accuracy of 500 μm. This is the max error allowed in terms of forcing the glass plate over the mould. The HYP mould is fixed to its mounting frame; the mould is spring preloaded against the frame corner and held down by a spring loaded screw.
	The PAR glass plate is mounted on its mould and held on it by vacuum suction; the alignment of the plate on its mould is done by markers with a typical accuracy of 500 μm. This is the max error allowed in terms of forcing the glass plate over the mould. The PAR mould is fixed to its mounting frame; the mould is spring preloaded against the frame corner and held down by a spring loaded screw.
	The UPMC is used to: (1) measure the two shells over the moulds to compute their position with respect to the moulds themselves; (2) scan the two moulds along their "parallels" edges; the accuracy of the UPMC over a 200mm range is 1 μm (after calibration) which gives an accuracy of 0.14'' for Ry" and 0.6'' about Rx". (3) measure the position X, Y, Z and the rotation Rz of the two moulds by probing the moulds surfaces in few points.
	The hexapod is commanded to place (position and attitude) the HYP mould. Hexapod repeatability: +/-10 mrad=2'', Min. incremental motion: +/-5 mrad=1''. (REQ: 20'' Par+Hyp)
	The 6 picomotors are commanded to correct the attitude of the PAR mould with respect to the HYP one.
	At this stage relative angles of the two moulds are measured by the two autocollimators placed aboard the integration bench.

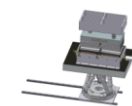
IMAGE**STEP DESCRIPTION**



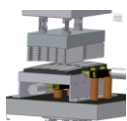
These two measures are recorded and eventually used during the integration phase to command the 6-axis mechanism to keep them constant. Now the position and attitude of the plates pair are known in the UPMC Coordinate System. The UPMC measures the position and attitude of the backplane.



The ribs are placed on the glass over the mould and prepared to be glued to the mirror module.



The IMA moves to the integration position under the mirror module mounting frame (possible tip-tilt error introduced by the linear guides <10" HYP+PAR)



The autocollimators are now used to check again the relative angles of the two moulds. The relevant corrections are commanded to the 6-axis mechanism to restore angles to their nominal values .



The hexapod places the glass plates pair in the gluing position which is determined on the base of the previously measured positions, leaving the desired glue thickness space. In this phase it is still possible to measure directly the position and attitude of the moulds. Therefore the positioning of the moulds pair under the XOU_B stack is always checked in closed loop by the UPMC. In particular this allows controlling with few microns precision the thickness left for the glue layer. Possible metrology of both the PAR and HYP plates with the CUP can be performed after gluing the couple.



Previous step is then repeated every TBD minutes to keep the mould correct attitude along the glue curing time. At a given point of the glue curing the vacuum suction is switched off to release the two shells and the IMA moves away (hexapod down).

Previous steps are repeated in order to glue the glass plate pair.

6. CONCLUSIONS

The plate pair integration scheme has been illustrated. This integration concept is robust and well understood. In particular, unlike the Pore Optics technology, no cumulative errors are expected as the common backplane is taken as reference for each PP and sources of systematic errors seems negligible. The corresponding error budget is under evaluation and a set of tolerances has been determined with ray-tracing simulations. Tolerances for more heuristic parameters will be assessed in the test campaign. Assuming the tolerances of the integration tools with contact probes already available, it seems feasible to meet the integration requirements. In any case an optical test and profile test to verify the focal position is still possible once the plates are integrated. Moreover, the possibility to un-glue a glass from the rib has been already successfully tested. IMA preliminary design is completed. In perspective the system can be fully automatable with robotic systems. The integration procedure is compatible with FMA design provided by BCV.

7. ACKNOWLEDGEMENT

This research is funded by ESA in the context of the contract "Back-up IXO (former XEUS) Optics Technology".

REFERENCES

- [RD1] M. J. Collon; S. Kraft; R. Günther; E. Maddox; M. Beijersbergen; M. Bavdaz; D. Lumb; K. Wallace; M. Krumrey; L. Cibik; M. Freyberg, "Performance characterization of silicon pore optics", Proc. SPIE, v. 6266, (2006)
- [RD2] W. Zhang, "Lightweight X-ray Mirrors for the Constellation-X Mission", Proc. SPIE, 6266-68, 2006.
- [RD3] M. Ghigo, S. Basso, R. Canestrari, P. Conconi, O. Citterio, M. Civitani, E. Dell'Orto, D. Gallieni, G. Pareschi, G. Parodi, L. Proserpio, D. Spiga, "Hot slumping glass technology and integration process to manufacture a grazing incidence scaled prototype for the IXO telescope modules", Proc. SPIE Vol. 7437-22, (2009)
- [RD4] M. Ghigo, S. Basso, P. Conconi, O. Citterio, M. Civitani, R. Negri, G. Pagano, G. Pareschi, L. Proserpio, B. Salmaso, F. Scaglione, D. Spiga, G. Tagliaferri, L. Terzi, A. Zambra, G. Parodi, F. Martelli, Gallieni, M. Tintori, P. Friedrich, M. Vongehr, A. Winter, M. Bavdaz, B. Guldemann, E. Wille, "Hot slumping glass technology for the grazing incidence optics of future missions, with particular reference to IXO", Proc. SPIE, 7732-11, (2010)
- [RD5] D. Spiga, "Analytical evaluation of the X-ray scattering contribution to imaging degradation in grazing-incidence X-ray telescopes". *Astronomy & Astrophysics* 468, 775-784 (2007)
- [RD6] M. Civitani, M. Ghigo, O. Citterio, L. Proserpio, D. Spiga, G. Pareschi, "3-D characterization of thin glass segmented X-ray mirrors via optical profilometry", To be submitted - Proc. SPIE Vol. 7803-19, (2010)